POLSKA AKADEMIA NAUK

INSTYTUT MASZYN PRZEPŁYWOWYCH

TRANSACTIONS OF THE INSTITUTE OF FLUID-FLOW MACHINERY

PRACE INSTYTUTU MASZYN PRZEPŁYWOWYCH

102

WYDAWNICTWO IMP PAN

GDAŃSK 1997

THE TRANSACTIONS OF THE INSTITUTE OF FLUID-FLOW MACHINERY

exist for the publication of theoretical and experimental investigations of all aspects of the mechanics and thermodynamics of fluid-flow with special reference to fluid-flow machines

*

PRACE INSTYTUTU MASZYN PRZEPŁYWOWYCH

poświęcone są publikacjom naukowym z zakresu teorii i badań doświadczalnych w dziedzinie mechaniki i termodynamiki przepływów, ze szczególnym uwzględnieniem problematyki maszyn przepływowych

Wydanie publikacji dofinansowane zostało przez PAN ze środków DOT uzyskanych z Komitetu Badań Naukowych

EDITORIAL OFFICE – REDAKCJA

Wydawnictwo Instytutu Maszyn Przepływowych
Polskiej Akademii Nauk
ul. Gen. Józefa Fiszera 14, 80-952 Gdańsk, skr. poczt. 621,
☎ (0-58) 46-08-81 wew. 141, fax: (0-58) 41-61-44,
e-mail: esli@imppan.imp.pg.gda.pl

ISSN 0079-3205

TRANSACTIONS OF THE INSTITUTE OF FLUID-FLOW MACHINERY
1997 No. 102

DARIUSZ P. MIKIELEWICZ[1]

Modelling of a buoyancy-influenced flow of supercritical pressure helium in a heated vertical pipe[2]

The work reports the results of the numerical simulations of the experiments performed on buoyancy-influenced ascending and descending flow of supercritical pressure helium in a heated vertical tube using the Launder and Sharma low-Reynolds number $k \sim \epsilon$ turbulence model. The response of the turbulence model has been found to be remarkably satisfactory under such severe conditions. However, the model is still not reliable enough to be recommended for the adequate modelling of the buoyancy-influenced flows.

Nomenclature

B	–	buoyancy parameter, $Gr/Re^{3.425}/Pr^{0.8}$,
c_p	–	specific heat capacity at constant pressure,
C_1, C_2	–	constants in modelled dissipation equation,
C_μ	–	constant in constitutive equation of eddy viscosity model,
D	–	term in low-Reynolds-number, k-equation, pipe diameter,
E	–	term in low-Reynolds-number
f_2	–	function in dissipation equation,
f_μ	–	function in constitutive equation of $k \sim \epsilon$ model,
g	–	acceleration due to gravity,
Gr	–	Grashof number, $\beta g D^4 q\bar{\mu}^2/\lambda/\mu^2$,
h	–	enthalpy,
k	–	turbulence kinetic energy,
Nu	–	Nusselt number, $q_w D/(T_w - T_b\lambda)$,
p	–	pressure,
Pr	–	Prandtl number, $C_p\mu/\lambda$,
q	–	wall heat flux,
r, z	–	cylindrical polar coordinates,
Re	–	Reynolds number, $\rho W_b D/\mu$,
Re_t	–	turbulence Reynolds number, $k^2/\nu\epsilon$,
t	–	time,
V, W	–	mean velocity in r, z directions,
y^+	–	non-dimensional distance from the wall,
ϵ	–	modified rate of dissipation of turbulence kinetic energy, $\tilde{\epsilon} = \epsilon - D$,
λ	–	thermal conductivity,
μ	–	dynamic viscosity,
ν	–	kinematic viscosity,
ρ	–	density,
σ_r	–	turbulent Prandtl number
$\sigma_k, \sigma_\epsilon$	–	turbulent Prandtl number for diffusion of k, ϵ.

[1]Institute of Fluid-Flow Machinery, Department of Thermodynamics and Heat Transfer, Fiszera 14, 80-952 Gdańsk
Present address: Technical University of Gdańsk, Heat Technology Department, Narutowicza 11/12, 80-952 Gdańsk

[2]The paper was sponsored by a research project KBN 3 P404 005 06

Subscripts

b – bulk, w – wall.
t – turbulent,

Abbreviations

LS – Launder and Sharma low-Reynolds $k \sim \epsilon$ model [2],

1. Introduction

In view of the complexity of the phenomenon of turbulence, its analysis and modelling present great difficulties. In recent years, there has been a great concentration of effort in industry on computational modelling of problems involving turbulent fluid flow and heat transfer, usually using codes of considerable versatility. It is sometimes mistakenly assumed that the turbulence models incorporated in such codes possess more universality than is the case and this can lead to incorrect usage of the codes and wrong conclusions being drawn from the results obtained. Particularly supercritical heat transfer numerical simulations demand superior knowledge of the turbulence model which is to be used. Therefore the role of throughout validation of the turbulence model based on empirical data is decisive in justification of a particular turbulence model.

Supercritical heat transfer has received much attention in recent years and there are several review articles [1-5] regarding the phenomena involved there. The main problem in supercritical heat transfer has always been perceived in the large property variations which occur near the critical point. Moreover, the effect of buoyancy forces, particularly in upflow in larger tubes, has been recognized and identified as the cause of the sharp deteriorations in heat transfer encountered under these conditions. Most of the papers dealt with the case of supercritical pressure carbon dioxide and water, less attention being paid to other supercritical pressure fluids. On one hand this could probably be attributed to the lack of accurate thermal property data, which is still not reliable enough for accurate numerical modelling.

In the buoyancy-aided heat transfer, heating of a thin layer of fluid near the pipe wall causes it to become buoyant. In such case this helps to overcome the shear force exerted by the wall on the fluid. As a result, the shear stress experienced by the fluid outside the buoyant layer is lower than it otherwise would be and the production of turbulence is reduced. The flow thus takes the characteristics of the flow corresponding to a lower flow rate having lower turbulence level. The greater the buoyancy influence, the more the turbulence is reduced. A stage is eventually reached where the force on the buoyant fluid is sufficient to completely overcome the wall shear. As a result, the core fluid does not experience any shear. Under such conditions the turbulence production will be switched off completely

and the flow can then be said to have become laminarised. Further increase of buoyancy leads to exerting the pressure in the opposite direction on the core fluid. This readily leads to recovery of turbulence production. With further increase of buoyancy influence, turbulence becomes more increased. The modification of the turbulence properties of the flow with build-up of buoyancy influence has a direct bearing on the effectiveness of heat transfer. Thus, with progressive increase of buoyancy influence, the heat transfer coefficient for upward flow in a heated vertical tube firstly becomes impaired, then falls to a minimum when the laminarisation stage is reached and subsequently recovers, eventually becoming enhanced. In descending flow the effect of buoyancy is in the opposite sense. As a result the turbulence is increased and the flow progressively takes the characteristics of the one corresponding to higher flow rates. Consequently, the heat transfer becomes progressively enhanced.

The author has already embarked on the path for searching a universal turbulence model which would be applicable to the cases of buoyancy influenced flows in vertical heated pipes [6]. From that work it had been concluded that the Launder and Sharma $k \sim \epsilon$ turbulence model [7] was the best of twelve other turbulence models used in modelling of buoyancy influenced flows. Hence, the author decided to test this model under conditions of buoyancy-influenced flow of supercritical pressure helium in heated vertical pipes. The experimental data reported by Brassington and Cairns [8] has been selected for validation of the model as the behaviour of the LS model has never been tested under such conditions. The data under consideration here contain the experiments of buoyancy-aided and buoyancy-opposed heat transfer in a heated vertical pipe. A particular feature of the data is that even though the values of the Reynolds number were high ($Re > 90000$), most results were strongly buoyancy influenced. At pressures above the critical value, the thermophysical properties of helium vary rapidly with temperature (and pressure, but to a lesser extent). Therefore, very significant variations of physical properties were present across the thermal layer. It was expected that variable property effects could even play more significant role than the buoyancy- influences because thermophysical properties of supercritical pressure helium vary very significantly in the considered region.

It is intended to test the ability the $k \sim \epsilon$ turbulence model due to Launder and Sharma to predict the flow of supercritical pressure helium in a vertical pipe with the account of the very strong variation of physical properties. The problem is axisymmetric and parabolic. This approach has already proved to be successful in the simulations of buoyancy-influenced wall shear flows of atmospheric pressure air in the papers of Cotton and Jackson [9,10], where the turbulence model of Launder and Sharma [7] was used to simulate experimental data [11-13]. Jackson and Mikielewicz [14-16] performed some comparative studies of turbulence models on the experimental data for air [17] and water [18] as a round-off of the work [6], where several $k \sim \epsilon$ turbulence models have been implemented in the computer code CONVERT. The code was originally developed by Cotton [19] and later modified by Yu [20] to include the effects of property variations. Mikielewicz [21-22] has further extended the code to include the number of turbulence

models. He also tested some other models on data from [17-18]. From all these works it appeared that only the LS model seemed to be capable to deal with the effects of buoyancy influence, but was strongly over-responding to the effects of property variation. Knowing these advantages and disadvantages of the LS model the author wanted to test it on a cryogenic fluid such as supercritical helium. This involves severe changes in thermal properties and it will be interesting to see how the model which is known to over-respond to the effect of property variation will behave in the case of this fluid.

2. Governing equations

The geometry considered here is the pipe flow and hence the governing equations are written in the 'boundary layer' approximation. The principal flow direction coincides with the axis of the pipe and the main gradients act in the direction normal to the axis. The thermal boundary condition of the second kind has been considered here, i.e. $q_w = const$. The governing equations read as follows:

continuity equation

$$\frac{1}{r}\frac{\partial(\rho r V)}{\partial r} + \frac{\partial(\rho W)}{\partial z} = 0, \tag{1}$$

momentum equation

$$\frac{1}{r}\frac{\partial(r\rho VW)}{\partial r} + \frac{\partial(\rho W^2)}{\partial z} = -\frac{dp}{dz} + \frac{1}{r}\frac{\partial}{\partial r}\left[r(\mu + \mu_t)\frac{\partial W}{\partial r}\right] \pm \rho g, \tag{2}$$

energy equation

$$\frac{1}{r}\frac{r\partial(\rho V h)}{\partial r} + \frac{\partial(\rho W h)}{\partial z} = \frac{1}{r}\frac{\partial}{\partial r}\left[r\left(\frac{\lambda}{C_p} + \frac{\mu_t}{\sigma_t}\right)\frac{\partial h}{\partial r}\right]. \tag{3}$$

After [23] the turbulent Prandtl number have been assigned a uniform value of 0.85.

3. Turbulence models

In order to solve the above equations the concept of turbulent viscosity is employed. In the case of the $k \sim \epsilon$ models the velocity scale is represented by the square root of the turbulence kinetic energy k and the turbulence length scale is the product of its rate of dissipation $\epsilon (= k^{3/2}/\epsilon)$. In low-Reynolds-number models, which are considered here, the transport equations are solved over the entire flow domain without recourse to wall functions. In the case of the $k \sim \epsilon$ model, the constitutive equation for the turbulent viscosity reads as follows:

$$\mu_t = C_\mu f_\mu \frac{\rho k^2}{\epsilon}. \tag{4}$$

The equations, which define transport of k and ϵ equations are as follows:
k-transport

$$\frac{1}{r}\frac{\partial(\rho r V k)}{\partial r} + \frac{\partial(\rho W k)}{\partial z} = \mu_t \left(\frac{\partial W}{\partial r}\right)^2 + \frac{1}{r}\frac{\partial}{\partial r}\left[r\left(\mu + \frac{\mu_t}{\sigma_k}\right)\frac{\partial k}{\partial r}\right] - \rho(\epsilon + D), \quad (5)$$

ϵ-transport

$$\frac{1}{r}\frac{\partial(\rho r V \epsilon)}{\partial r} + \frac{\partial(\rho W \epsilon)}{\partial z} = C_1 \frac{\epsilon}{k}\mu_t \left(\frac{\partial W}{\partial r}\right)^2 + \frac{1}{r}\frac{\partial}{\partial r}\left[r\left(\mu + \frac{\mu_r}{\sigma_\epsilon}\right)\frac{\partial \epsilon}{\partial r}\right] -$$

$$-C_2 f_2 \frac{\rho\epsilon^2}{k} + \frac{2\mu\mu_t}{\rho}\left(\frac{\partial^2 W}{\partial y^2}\right)^2. \quad (6)$$

The model considered here has the form that when f_μ and f_2 are set to unity, and terms D and E are set to zero, the standard high-Reynolds version of the $k \sim \epsilon$ model is retrieved. Tables 1 and 2 present details of functions and constants incorporated in the $k \sim \epsilon$ model used.

Table 1. Damping functions and model terms used in the model

Model	f_2	f_μ	D	E
LS	$1.0 - 0.3\exp(-Re_t^2)$	$\exp\left[\frac{-3.4}{(1+Re_t/50)^2}\right]$	$2\mu\left(\frac{\partial\sqrt{k}}{\partial y}\right)^2 \quad y^+ \le 2$ $\frac{2\mu k}{y^2} \quad y^+ > 2$	$\frac{2\mu\mu_t}{\rho}\left(\frac{\partial^2 W}{\partial y^2}\right)^2$

Table 2. Model constants

Model	C_μ	C_1	C_2	σ_k	σ_ϵ
LS	0.09	1.44	1.92	1.0	1.3

The boundary conditions used in the solution of the k and ϵ equations are: $k = 0$ and $\epsilon_w = 0$.

4. Results

Local heat transfer measurements were obtained using a uniformly heated 17.8mm bore HT9 aluminium alloy drawn tube of wall thickness of 1.6mm. The test section had an unheated entry length of 24 diameters which was followed

by a heated length of 55 diameters. As the authors of the data say, for various reasons mainly concerned with avoiding excessive boil-off from the helium bath it was not possible to maintain constant test-section inlet conditions. Hence the results consisted of hundreds of wall temperature profiles taken at fairly random values of inlet temperature, pressure, flow rate and heat input. Data were collected for Reynolds numbers in the range from 90000 to 700000 and the buoyancy parameter B ($B = 80000Gr^*/Re^{3.425}/Pr^{0.8}$), which was introduced by Hall and Jackson [28] and Jackson and Hall [29], in the range from $9.0 \cdot 10^{-9}$ to $9.9 \cdot 10^{-6}$.

As mentioned earlier, the conditions described here involve significant property variations. The thermophysical properties of supercritical pressure helium have been taken from the tabulated data by McCarty [24] and were both temperature and pressure dependent. The tables of density, dynamic viscosity, thermal conductivity and specific heat were subsequently incorporated into the code. In order to calculate a particular thermophysical property, a two-dimensional (temperature and pressure) bicubic spline was calculated at each profile point. This led to very extensive computing time. On average, the run performed took about 60 hours on the SPARC20 SUN machine (which is on average four times faster than the PC486/66DX2.

The thermal resistance of the wall layer will in this case be modified due to the variation of thermal conductivity and Prandtl number. Firstly, the increase in thermal conductivity in the wall layer with increase of temperature will cause the thermal resistance of the viscous sub-layer to decrease. Another important effect arises because of the variation of the Prandtl number (which decreases with temperature). This will decrease the turbulent conductivity ($= kPr/\sigma_t\mu_t/\mu$) and this will increase the effective thickness of the wall layer (an opposite effect). These effects will combine with the effect of viscosity increase in near-wall damping, which is known from [6] to be vastly overestimated by the LS model to cause it to over-predict the heat transfer coefficient.

4.1. Ascending flow simulations

For the purpose of the present report a representative sample of three upflow runs have been selected as a subset of data reported in [8]. The runs are of a similar Reynolds number which ranged from 91000 to 96000. The inlet buoyancy parameter ranged from $7.3 \cdot 10^{-6}$ to $9.9 \cdot 10^{-6}$. These parameters correspond to the conditions beyond the maximum impairment of heat transfer. The experimental data have been presented on the basis of the development of the wall temperature (not in run 3) and heat transfer coefficient. Figs. 1 to 6 present the respective runs.

From the figures we can see that the LS model responds strongly to the influences of buoyancy and variable properties. The wall temperature distribution calculated by the model does not closely reproduce the experimental one but the general behaviour is quite satisfactory. The wall temperature peak and subsequent trough (an indication of partial laminarisation and the start of recovery of heat transfer respectively) both in the experiment and simulations are coinciding

but their magnitudes are different. The simulated peaks are flatter and extend for over 10 diameters whereas in experiment these are a clear sharp peaks. Some of that rather irregular behaviour in the LS model simulations can probably be attributed to the Prandtl number variation effects in the wall layer (augmentation of the effective thickness of the thermal layer).

In [6] it had been found that the LS model is rather very sensitive to the physical property variations. When we focus our attention on the development of the heat transfer coefficient (see Figs. 2, 4 and 6) some of the observed behaviour can be devoted to this fact. After the partial laminarisation of the flow the heat transfer recovers to reach some maximum (common for experiment and simulation). Then later, the heat transfer coefficient starts to deteriorate at a some small rate. This behaviour is revealed by the experimental data and numerical simulation, but in the case of the predictions it deteriorates at much faster rate. In all experiments a clear maximum forms after about 20 diameters depending on the buoyancy parameter. It is rather easy to explain why the maximum occur at the same location as in all these cases the buoyancy parameter takes a similar value at this point. The heat transfer coefficient then deteriorates in the case of the numerical experiment. Such a behaviour has also been found earlier in the case of other fluids at normal conditions simulated by the author in [6]. This phenomenon was named as a secondary laminarisation. It was thought that the deterioration of the heat transfer coefficient arises by the virtue of property effects. The discrepancy between the experiment and numerical simulation is increasing with the increase of the wall-to-bulk temperature difference. In the case of run 2 (Figs. 3 and 4), there is a formation of a second maximum after about 45 diameters. This is the case for the simulation only as in the experiment the heat transfer coefficient reduces steadily. The author suspects that a similar mechanism to that when the maximum of heat transfer is reached is also involved in this case. The secondary laminarisation by virtue of property variation has already been developing and at this stage the recovering turbulence production (damped by the secondary laminarisation) starts to overcome the reduction of the heat transfer coefficient by means of variable property effects. This is only possible because the wall-to-bulk temperature difference is biggest in the case of this run and the secondary laminarisation is more severe.

In order to dissect the anatomy of the flow some radial profiles have been generated of the Reynolds stress, turbulence kinetic energy and the dissipation of kinetic energy at different axial locations. These are presented in Figs. 7 to 10.

In Figs. 7 and 8, we can observe the changes of the Reynolds stress at various longitudinal positions. In [6], it has been found that in the case of the LS model the turbulence production ceased in the near wall region when the conditions of partial laminarisation of the flow had been encountered. This was reflected by the disappearance of the Reynolds stress near the wall. The subsequent recovery could not take place as within the flow there was not enough turbulence to help the Reynolds stress recovery. The slightly different pattern of the Reynolds stress modifications holds here. The Reynolds stress disappears very close to the wall prior to reaching laminarisation position (Fig. 8, $z/D = 5$), but starting there

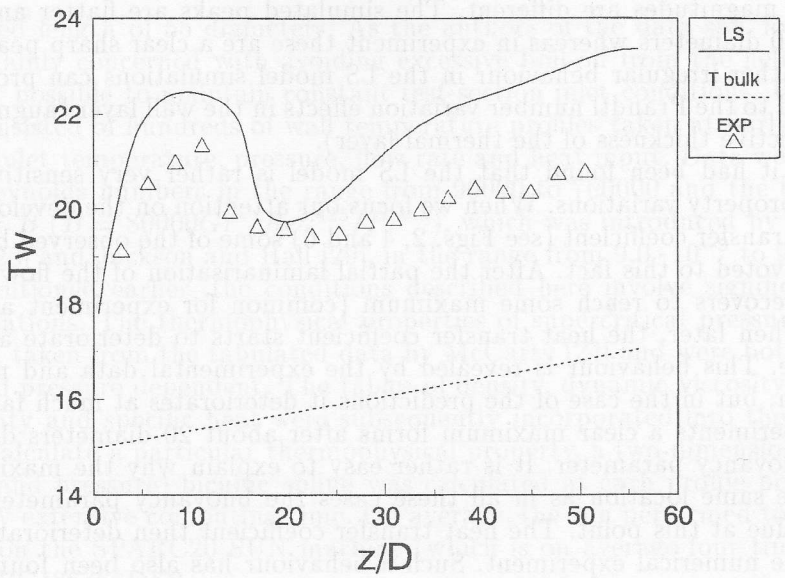

Fig. 1. Wall and bulk temperature development, inlet conditions: Re=91000, Gr=$6.228 \cdot 10^{11}$, Pr=0.828, B=$7.355 \cdot 10^{-6}$.

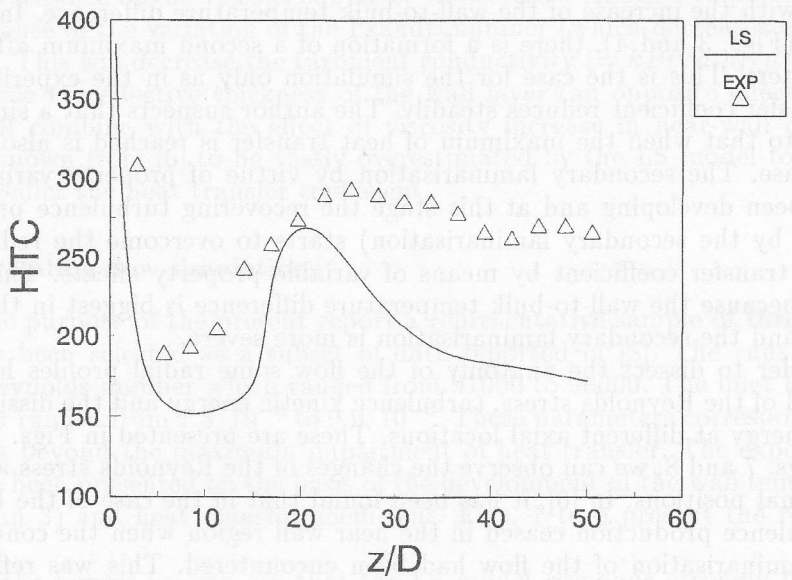

Fig. 2. Heat transfer coefficient development, inlet conditions: Re=91000, Gr=$6.228 \cdot 10^{11}$, Pr=0.828, B=$7.355 \cdot 10^{-6}$.

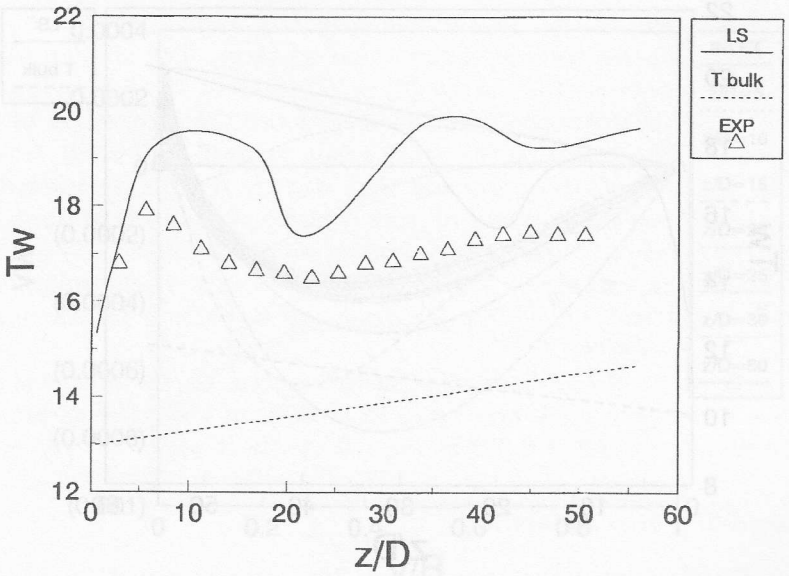

Fig. 3. Wall and bulk temperature distribution, inlet conditions: Re=96000, Gr=$8.171 \cdot 10^{11}$, Pr=0.860, B=$7.788 \cdot 10^{6}$.

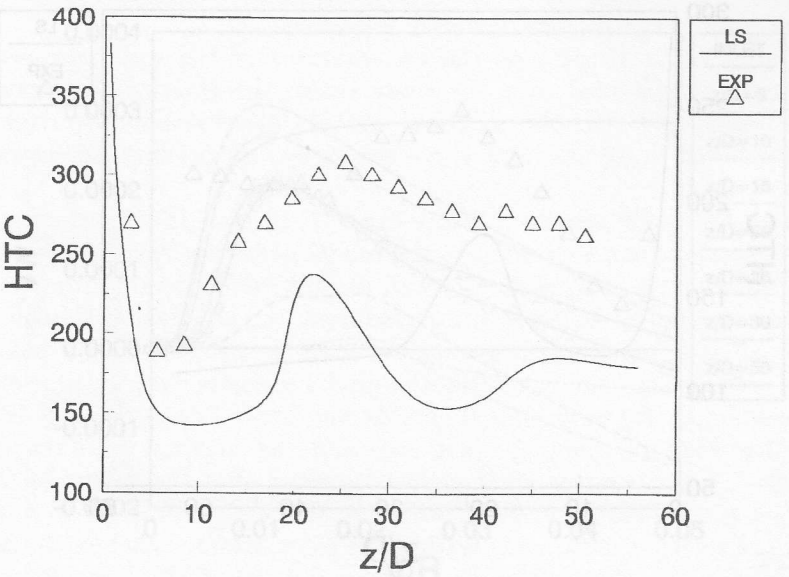

Fig. 4. Heat transfer coefficient development, inlet conditions: Re=96000, Gr=$8.171 \cdot 10^{11}$, Pr=0.860, B=$7.788 \cdot 10^{-6}$.

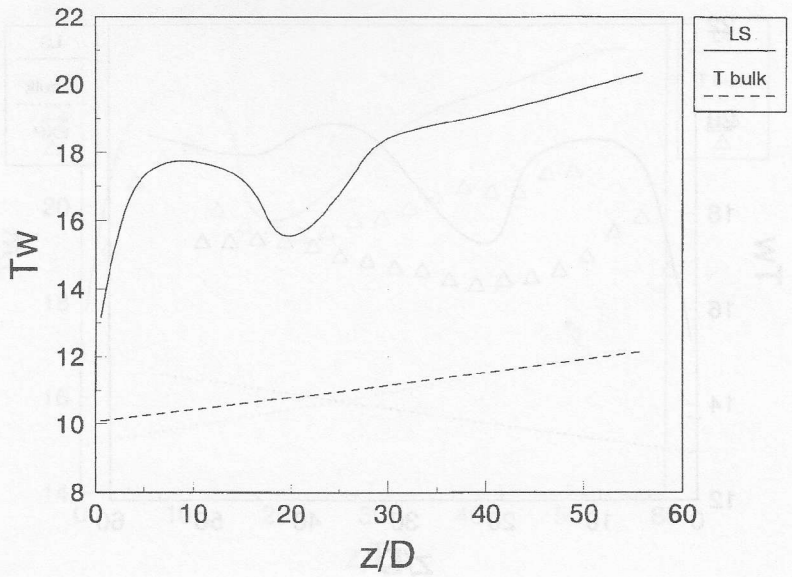

Fig. 5. Wall and bulk temperature development, inlet conditions: Re=95000, Gr=$1.072 \cdot 10^{12}$, Pr=0.921, B=$9.934 \cdot 10^{-6}$.

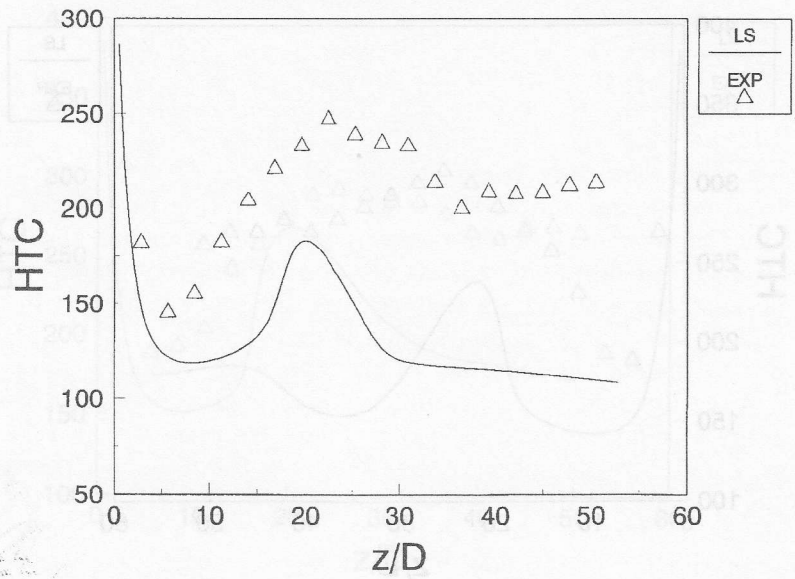

Fig. 6. Heat transfer coefficient distribution, inlet conditions: Re=95000, Gr=$1.072 \cdot 10^{12}$, Pr=0.921, B=$9.934 \cdot 10^{-6}$.

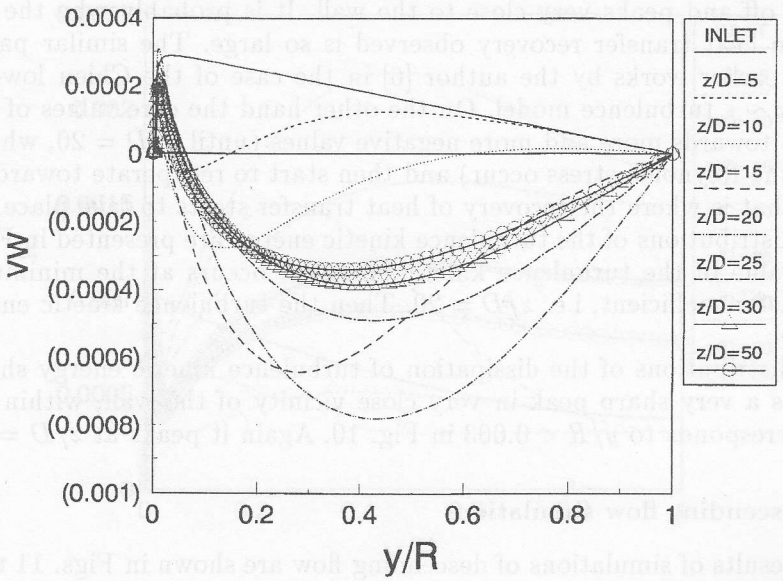

Fig. 7. Distributions of Reynolds stress, inlet conditions: Re=91000, Gr=$6.228 \cdot 10^{11}$, Pr=0.828, B=$7.355 \cdot 10^{-6}$.

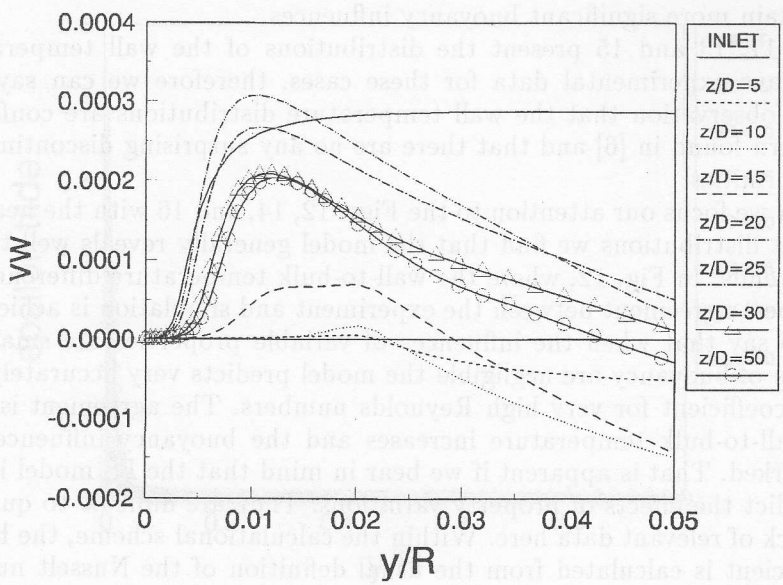

Fig. 8. Distributions of Reynolds stress, inlet conditions: Re=91000, Gr=$6.228 \cdot 10^{11}$, Pr=0.828, B=$7.355 \cdot 10^{-6}$.

it shoots off and peaks very close to the wall. It is probably why the extent to which the heat transfer recovery observed is so large. The similar pattern was found in earlier works by the author [6] in the case of the Chien low-Reynolds number $k \sim \epsilon$ turbulence model. On the other hand the core values of the stress tend first towards more and more negative values (until $z/D = 20$, where lowest value of the Reynolds stress occur) and then start to recuperate towards positive values. That is where the recovery of heat transfer starts to take place.

The distributions of the turbulence kinetic energy are presented in Fig. 9. The highest value of the turbulence kinetic energy k occurs at the minimum of the heat transfer coefficient, i.e. $z/D = 20$. Then the turbulence kinetic energy start to reduce.

The distributions of the dissipation of turbulence kinetic energy shows up in Fig. 10 as a very sharp peak in very close vicinity of the wall, within $y^+ < 15$, which corresponds to $y/R < 0.003$ in Fig. 10. Again it peaks at $z/D = 20$.

4.2. Descending flow simulations

The results of simulations of descending flow are shown in Figs. 11 to 16. The Reynolds number ranges from 115000 to 710000. The buoyancy parameter takes values from $9.0 \cdot 10^{-9}$ to $4.3 \cdot 10^{-6}$. The first condition corresponds to the condition of virtually forced convection with no buoyancy influence. It is not surprising as the Reynolds number in this case is very high ($Re = 710000$). Two remaining ones contain more significant buoyancy influences.

Figs. 11, 13 and 15 present the distributions of the wall temperature. We do not have experimental data for these cases, therefore we can say no more than the observation that the wall temperature distributions are conforming to the pattern found in [6] and that there are no any surprising discontinuities and non-uniformities.

When we focus our attention to the Figs. 12, 14, and 16 with the heat transfer coefficient distributions we find that the model generally reveals well the experimental trends. In Fig. 12, where the wall-to-bulk temperature difference is smallest the best agreement between the experiment and simulation is achieved. That allows to say that when the influences of variable properties are small and the influences of buoyancy are negligible the model predicts very accurately the heat transfer coefficient for very high Reynolds numbers. The agreement is less good if the wall-to-bulk temperature increases and the buoyancy influence becomes more marked. That is apparent if we bear in mind that the LS model is prone to over-predict the effects of property variations. They are difficult to quantify due to the lack of relevant data here. Within the calculational scheme, the heat transfer coefficient is calculated from the usual definition of the Nusselt number and hence, the thermal property which triggers the influences of property variations to become present is the thermal conductivity ($h = Nu \cdot k/d$). In Figs. 14 and 16 we can observe some non-uniformity in the experimental distribution of the heat transfer coefficient. This is confirmed by the model only in Fig. 16 but only qualitatively. This is the interaction between the thermal development of the flow

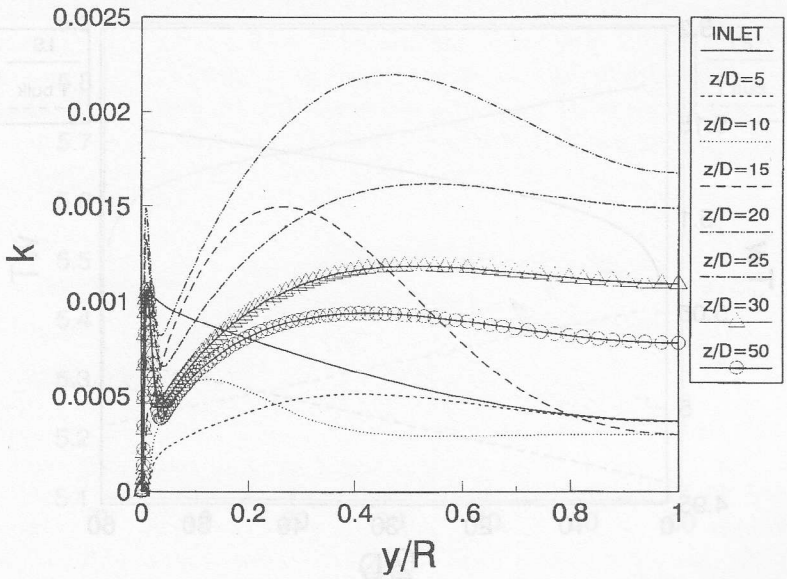

Fig. 9. Distributions of the turbulence kinetic energy, inlet conditions: Re=91000, Gr=$6.228 \cdot 10^{11}$, Pr=0.828, B=$7.355 \cdot 10^{-6}$.

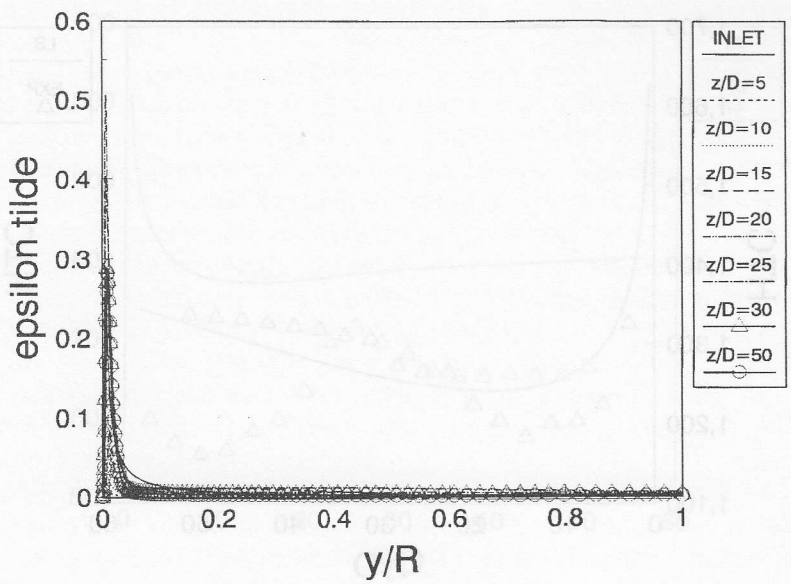

Fig. 10. Distributions of dissipation of turbulence energy, inlet conditions: Re=91000, Gr=$6.228 \cdot 10^{11}$, Pr=0.828, B=$7.355 \cdot 10^{-6}$.

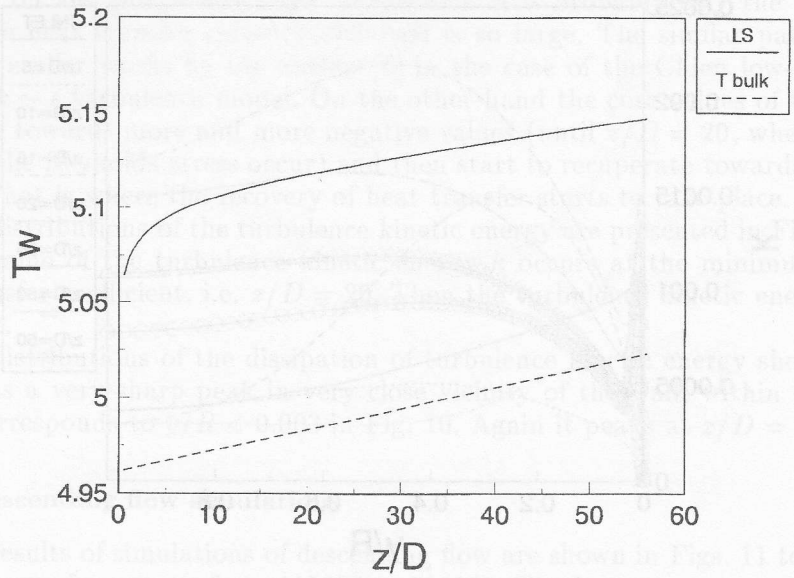

Fig. 11. Wall and bulk temperature development, inlet conditions: Re=710000, Gr=7.252·10^4, Pr=0.678, B=9.0·10^{-9}.

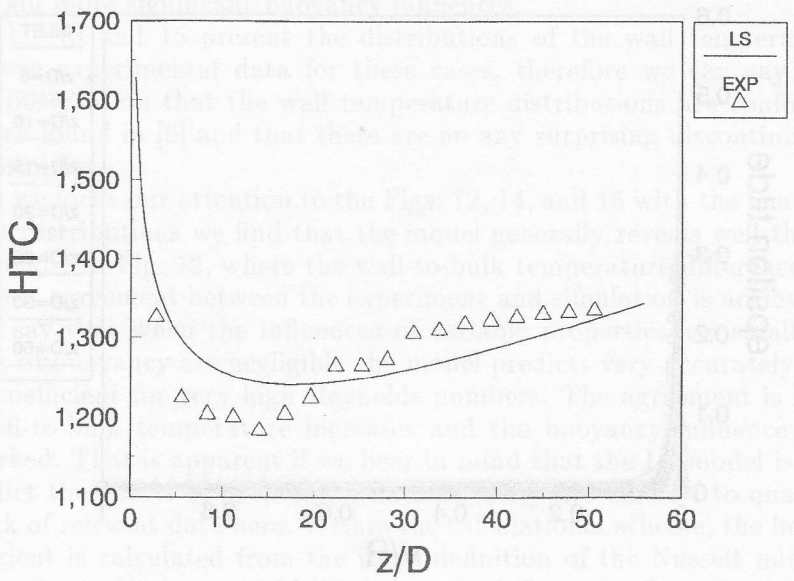

Fig. 12. Heat transfer coefficient distribution, inlet conditions: Re=710000, Gr=7.252·10^4, Pr=0.678, B=9.0·10^{-9}.

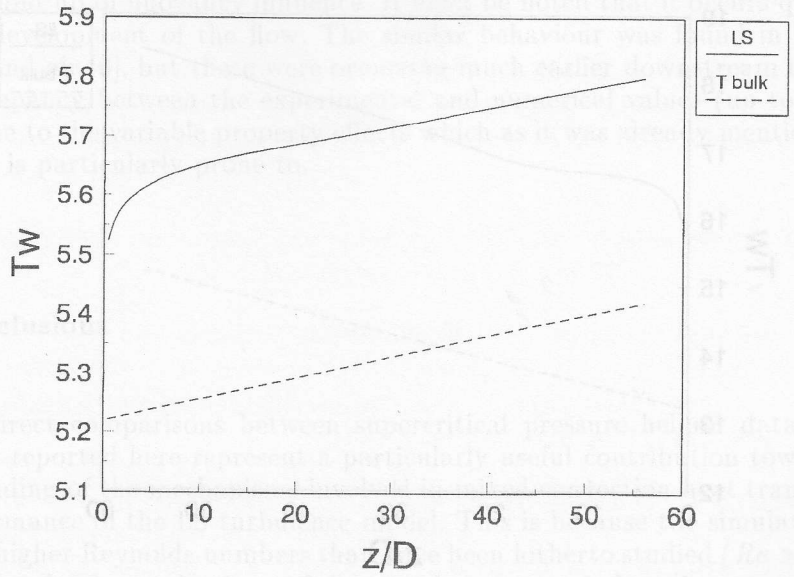

Fig. 13. Wall and bulk temperature development, inlet conditions: Re=330000, Gr=$2.463 \cdot 10^{12}$, Pr=0.758, B=$3.76 \cdot 10^{-6}$.

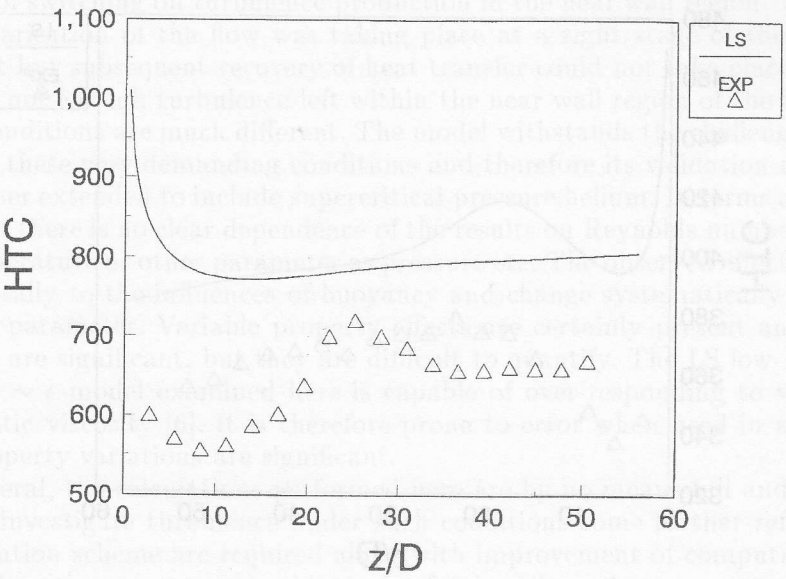

Fig. 14. Heat transfer coefficient distribution, inlet conditions: Re=330000, Gr=$2.463 \cdot 10^{12}$, Pr=0.758, B=$3.76 \cdot 10^{-6}$.

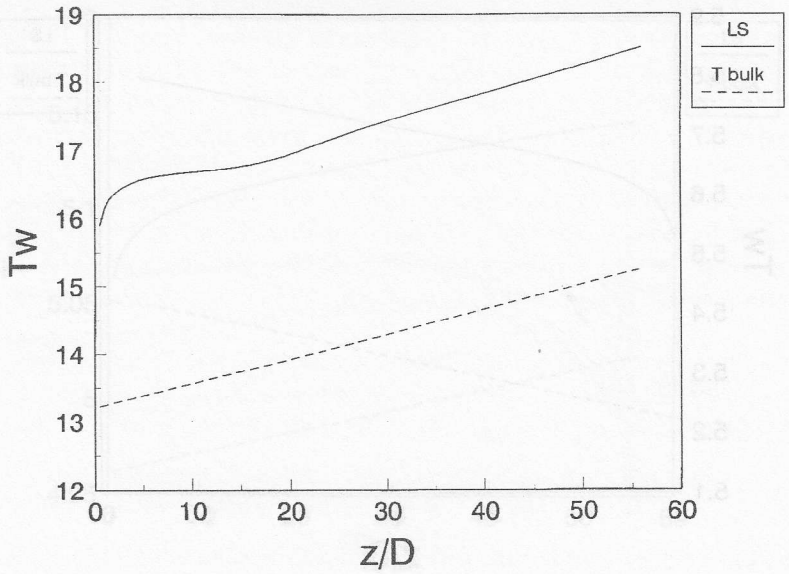

Fig. 15. Wall and bulk temperature development, inlet conditions: Re=115000, Gr=$8.364 \cdot 10^{11}$, Pr=0.847, B=$4.333 \cdot 10^{-6}$.

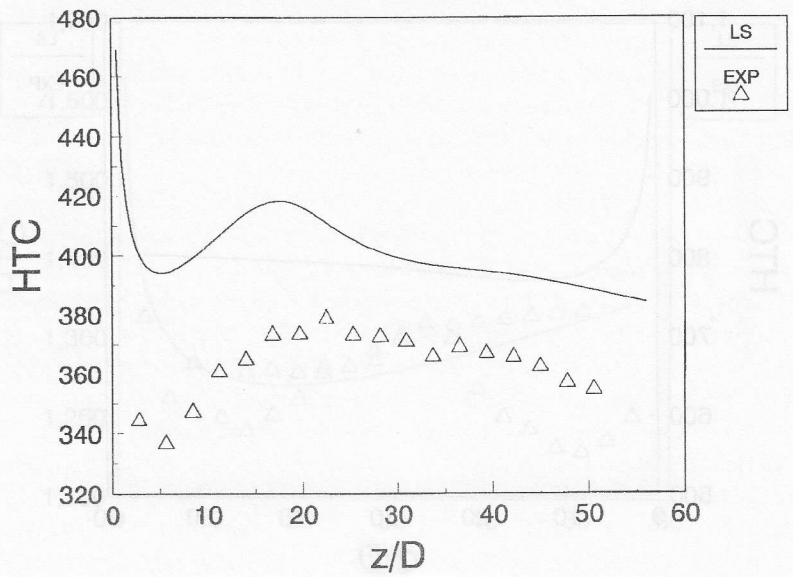

Fig. 16. Heat transfer coefficient development, inlet conditions: Re=115000, Gr=$8.364 \cdot 10^{11}$, Pr=0.847, B=$4.333 \cdot 10^{-6}$.

and the build up of buoyancy influence. It must be noted that it occurs quite well into the development of the flow. The similar behaviour was found in the case of water and air [6], but these were occurring much earlier downstream the pipe. The discrepancy between the experimental and numerical values (up to 25%) is mainly due to the variable property effects which as it was already mentioned the LS model is particularly prone to.

5. Conclusions

The direct comparisons between supercritical pressure helium data and simulations reported here represent a particularly useful contribution towards the understanding of the mechanisms involved in mixed convection heat transfer and the performance of the LS turbulence model. This is because the simulations are for much higher Reynolds numbers than have been hitherto studied ($Re > 91000$). In earlier works the mechanisms of the model performance have been investigated under moderate and small Reynolds numbers. The LS turbulence model responds to the influences of buoyancy very strongly but the picture is clouded by the presence of the variable property effects. Under such conditions the model worked on the basis of switching off turbulence production in the near wall region. Therefore the laminarisation of the flow was taking place at a right stage of the flow development but subsequent recovery of heat transfer could not take place because there was not enough turbulence left within the near wall region of the flow. The present conditions are much different. The model withstands the challenge of such testing at these very demanding conditions and therefore its validation range has been further extended to include supercritical pressure helium. In terms of general behaviour, there is no clear dependence of the results on Reynolds number or bulk inlet temperature or other parameter as pressure etc. The observed effects are due fundamentally to the influences of buoyancy and change systematically with the buoyancy parameter. Variable property effects are certainly present and in certain cases are significant, but they are difficult to quantify. The LS low-Reynolds number $k \sim \epsilon$ model examined here is capable of over-responding to variations of kinematic viscosity [6]. It is therefore prone to error when used in situations where property variations are significant.

In general, the calculations performed here are by no means full and in order to better investigate turbulence under such conditions some further refinements to the solution scheme are required along with improvement of computing facilities in order to generate more evidence for further discussion.

In downward flow, the general trend of enhancement of heat transfer due to buoyancy is reproduced by the model. However, the calculated relative heat transfer could be misleading due to the limitations of the model in terms of over-prediction of the variable property effects.

Acknowledgements

The support of the Polish Scientific Committee for Research grant No. 3 P404 005 06 is greatly acknowledged. The author wishes to express his thanks to Dr E. Ihnatowicz for his help in performing calculations to this work.

Manuscript received in December 1995

References

[1] Polyakov A.F.: *Heat Transfer under supercritical pressures*, Advances in Heat Transfer, Vol. 21, Academic Press, 1991

[2] Jackson J.D. and Hall W.B.: *Forced convection heat transfer to fluids at supercritical pressure*, Turb. in: Forced Convection in Channels and Bundles, Theory and Application to Heat Exchanger and Nuclear Reactor, 2, Adv. Study Inst. Book (eds. Kakac S. and Spalding D.B.), 1979.

[3] Hall W.B. and Jackson J.D.: *Heat transfer near the critical point*, Keynote Lecture, Proc. 6th Int. Heat Transfer Conference, Toronto, Canada, 1978.

[4] Jackson J.D.: *Studies of interaction by free and forced convection in vertical heated pipe flow*, National Heat Transfer Conference, UMIST, Manchester, 1995.

[5] Jackson J.D., Cotton M.A. and Axcell B.P.: *Studies of mixed convection in vertical tubes*, Int. J. Heat Fluid Flow, 10(1989), 2-15.

[6] Mikielewicz D.P.: *Comparative studies of turbulence models under conditions of mixed convection with variable properties in heated vertical tubes*, Ph.D. Thesis, University of Manchester, 1994.

[7] Launder B.E. and Sharma B.I.: *Application of the energy-dissipation model of turbulence to the calculation of flow near a spinning disc*, Lett. Heat Mass Transfer, 1(1974), 131-138.

[8] Brassington D.J. and Cairns D.N.H.: *Measurements of forced convective heat transfer to supercritical helium*, Int. J. Heat Mass Transfer, 20(1977), 207-214.

[9] Cotton M.A. and Jackson J.D.: *Vertical tube air flows in the turbulent mixed convection regime calculated using a low-Reynolds-number $k \sim \epsilon$ model*, Int. J. Heat Mass Transfer, 33(1990), 275-286.

[10] M.A. Cotton, Jackson J.D. and Yu L.S.L.: *Low-Reynolds-number $k \sim \epsilon$ simulations of turbulent mixed convection air flows in vertical pipes: inclusion of variable property effects*, submitted to Int. J. Heat Mass Transfer, 1995.

[11] Carr A.D., Connor M.A. and Buhr H.O.: *Velocity, temperature and turbulence measurements in air for pipe flow with combined free and forced convection*, J. Heat Transfer, 95(1973), 445-452.

[12] Steiner A.: *On the reverse transition of a turbulent flow under the action of buoyancy forces*, J. Fluid Mechanics, 47(1971), 503-512.

[13] Polyakov A.F. and Shindin S.A.: *Development of turbulent heat transfer over the length of vertical tubes in the presence of mixed air convection*, Int. J. Heat Mass Transfer, 31(1988).

[14] Jackson J.D. and Mikielewicz D.P.: *Computational studies of buoyancy-influenced flow of air in a vertical pipe*, Proc. Int. Symp. on Engineering Turbulence Modelling and Measurements, Crete, May 1996.

[15] Jackson J.D., Mikielewicz D.P. and Poskas P.: *Comparative study of turbulence models against some recent experimental data on buoyancy-influenced heat transfer for ascending flow od air in a tube*, Eurotherm No. 32, Oxford University, 1993.

[16] Jackson J.D., Mikielewicz D.P. and Buyukalaca O.: *Simulation of turbulent convective heat transfer to water in a vertical pipe*, IX Sympozjum Wymiany Ciepła i Masy, Augustów, 1995.

[17] Vilemas J.V., Poskas P.S. and Kaupas V.E.: *Local heat transfer in a vertical gas-cooled tube with turbulent mixed convection and different heat fluxes*, Int. J. Heat Mass Transfer, 35(1992), 2421-2428.

[18] Buyukalaca O.: *Studies of convective heat transfer to water in steady and unsteady pipe flow*, Ph.D. Thesis, University of Manchester, 1993.

[19] Cotton M.A.: *Theoretical studies of mixed convection in vertical tubes*, Ph.D. Thesis, University of Manchester, 1987.

[20] YuL.S.L.: *Computational studies of mixed convection in vertical pipes*, Ph.D. Thesis, University of Manchester, 1991.

[21] Mikielewicz D.P.: *Modelling a vertical pipe flow in descending flow of water*, Internal Report IMP PAN, No. 261/95, 1995.

[22] Mikielewicz D.P.: *Modelling an ascending flow of air in a heated vertical pipe*, Transactions of the Institute of Fluid-Flow Machinery, 101(1996), 89-104.

[23] Mikielewicz D.P. and Ihnatowicz E.: *Turbulence modelling using various turbulent Prandtl number*, Transactions of Institute of Fluid-Flow Machinery, 100(1996), 141-154.

[24] McCarty R.D.: *New equation of state, in NBS Report 10573*, Helium Heat Transfer, 1972.

[25] Hall W.B. and Jackson J.D.: *Laminarization of a turbulent pipe flow by buoyancy forces*, ASME Paper, 69-HT-55, 1969.

[26] Jackson J.D. and Hall W.B.: *Influences of buoyancy on heat transfer to fluids flowing in vertical tubes under turbulent conditions*, in: Turb. Forced Convection in Channels and Bundels, Theory and Application to Heat Exchanger and Nuclear Reactor, 2, Adv. Study Inst. Book (eds. Kakac S. and Spalding D.B.), 1979.

Modelowanie przepływu helu w warunkach ciśnień ponadkrytycznych w zakresie konwekcji mieszanej w pionowej rurze z grzaniem

Streszczenie

W niniejszej pracy przedstawiono wyniki bezpośrednich porównań symulacji numerycznych, przy użyciu modelu turbulencji Laundera i Sharmy z grupy $k \sim \epsilon$, z danymi eksperymentalnymi dotyczącymi przepływu w ramach konwekcji mieszanej helu w warunkach ciśnień ponadkrytycznych, w grzanej pionowej rurze. Symulacje przeprowadzone były przy uwzględnieniu zmienności własności fizycznych płynu. Otrzymane w wyniku obliczeń rezultaty przeprowadzonych za pomocą rozważanych modeli były satysfakcjonujące, aczkolwiek badania modelowe przepływów w takich warunkach są nadal wskazane.